BLADDER EXPANDABLE ROBOTIC SYSTEM AND UV MATERIALS FOR RAPID INTERNAL PIPELINE REPAIR

John J. Tierney[1], Alex Vanarelli[1], Jesse Brown[1], Lukas Fuessel[1], Ahmad Abu-Obaid[1], Steve Sauerbrunn[1], Shagata Das[1,2], Joseph Deitzel[1], Jovan Tatar[2], Dirk Heider[1], Harry W. Shenton III[2], Christopher J. Kloxin[4], Dae Han Sung[3], Erik Thostensen[13], John W. Gillespie Jr. [1234]

[1]Center for Composite Materials, [2]Civil and Environmental Engineering
[3]Mechanical Engineering, [4]Materials Science & Engineering
University of Delaware, Newark, DE, 19716, USA

ABSTRACT

This paper describes a novel composite placement process to fabricate stand-alone structural pipe within existing legacy pipelines—with no disruption in gas service. The process utilizes low-cost, UV-curable, glass fiber reinforced plastics (GFRP) for discrete preforms made from continuous fiber fabrics. These sections are designed to meet 50-year service life by addressing the unique loading conditions of the pipe repair allowing for the design customization of the preforms to accommodate the state of pipe corrosion, access points or other local features that may vary along the length of the pipe. The approach offers maximum design flexibility and customization while minimizing installation time and cost. The preforms are fabricated above ground using rapid automated manufacturing methods for quality control. The preforms are transported by a tethering system to the robot. The robot is comprised of a self-propelled dual inflation expandable bladder system that places, consolidates, and cures standard or custom composite sections along the entire pipe length in a continuous co-cure process. This system is designed to adapt to pipe features that include lateral tees, service connections, joints, gaps, and irregular cross sections. In addition, variable thickness composite sections can be placed along the pipe where exposed to high external loads under railroads, highways, airports or where soil erosion and movement occurs. This paper presents the robot design, assessment of UV curable resins, embedded sensing methods, and fabrication of pipe sections with this system.

Keywords: Pipeline repair, composite liner, robotic placement, UV cure
Corresponding author: John W. Gillespie Jr.

1. INTRODUCTION

Natural gas pipelines play a vital role in distributing gas with more than 1.2 million miles of distribution mains in the US. Iron and bare steel pipelines (legacy pipes) have been in operation since the 1940s [1] [2] with some even older. The Advanced Research Project Agency-Energy (ARPA-E) estimates approximately 20,000 miles of cast iron and 40,000 miles of bare steel pipes in the inventory. Legacy pipes have been a focus of replacement programs as they disproportionally have higher leak rates creating operational risk and reduce transmission efficiency increasing delivery cost [3] to the gas customer. Replacement of legacy pipes requires

SAMPE Conference Proceedings. Seattle, WA, April 17-20, 2023. Society for the Advancement of Material and Process Engineering – North America.

(DOI will be added by SAMPE)

excavation, and creates secondary societal costs (customer reconnect, congestion, road restoration, etc.). Pipe in pipe (PIP) repair is a commonly used rehabilitation approach but requires shutoff of gas services and restart costs with safety implications [4] [5]. Replacement costs are estimated to be around $2-$3 billion per year due to corrosion of these pipelines [6]. Our team (University of Delaware – Center for Composite Materials (UD-CCM) addresses this challenge by developing a PIP pipe in pipe repair system that does not require excavation and replacement of the legacy pipes. Our approach allows cost reduction projections well below $1 million per mile ARPA-E goal and has minimum operational impact on gas customers.

The UD-CCM project creates the novel material and robotic placement process to fabricate structural pipe within the existing pipelines without disruption of gas delivery. This paper describes the overall pipe design and provides results for the UV cured materials and mechanical properties, embedded sensors for gas leak detection and the development of the robot that incorporates the UV transparent bladder design for consolidation and UV lights for rapid cure at buried pipe operating temperatures. The feasibility of the system is demonstrated on 300mm (12-inch) diameter pipe sections. The repair process involves the delivery, expansion consolidation and UV cure of discrete composite preforms using a traveling robotic system. Straight and slightly curved pipe sections are bladder placed at high rate followed by repair of joints and steep bends using custom preform sections. The composite preforms are consolidated in place using a conformable robot and UV transparent annulus bladder that creates a stand-alone structural pipe within the legacy pipeline without the need for pipe shutdown. This process can operate in a hot pipe (running gas) environment that does not require shutdown of gas services due to the segmented delivery and open robotic support frame. It also doesn't require a structurally sound pipe wall as a support substrate due to the self-reacting hoop wound composite allowing for repair of compromised or unsupported pipe sections.

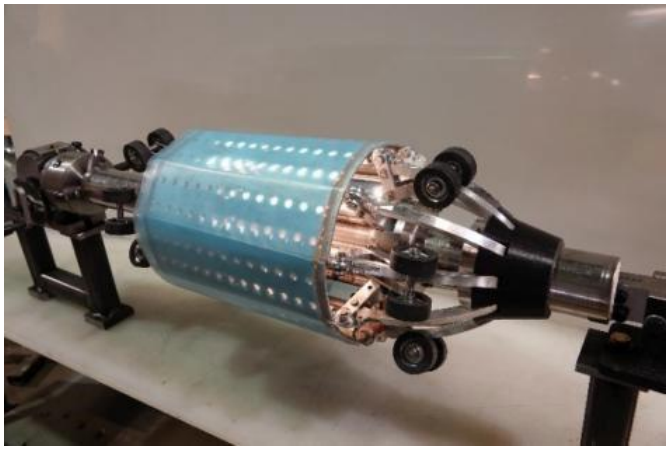

Figure 1 An articulating robot is expandable and incorporates an inflatable UV transparent bladder (light blue) with an integral array of UV LED lights (shown as axial rows placed around the circumference).

The preform material (prefabricated as an impregnated fabric in a cylindrical preform, vacuum sealed and collapsed to a smaller diameter package) is supplied nonstop using a tethered material feeding system and is placed, consolidated and UV cured with the robot as shown in Figure 2. This provides maximum placement efficiency reducing repair time and cost for straight sections. Each preform of finite length is co-cured with then next segment using a highly efficient scarf joint. and co-cured to the already repaired straight section. Two ingress/egress locations are

hot tapped to enable the repair process without shutdown and with minimal disruption to gas flow. The gas tapping processes exists commercially and is not a focus of this effort [7]. An inspection and mapping robot system will provide a complete mapping of the pipe that is used to define the composite manufacturing roadmap for pipeline rehabilitation strategy and geometric information for composite preform design and fabrication. Location, segment lengths and diameters of straight pipe sections are identified as well as compromised sections that require significant repair. Other regions with complex geometric features such as tight bends, joints or step-changes in diameter are also mapped.

In a second step, the self-propelled robotic system is inserted at the egress location and is supplied by discrete composite segments from the ingress location carried on collapsible spiders (Figure 2). Two spiders carry each segment to the robot using a pass-through tether that is pulled from the egress surface. The spiders are automatically collapsed by the robot nose and pass through the core of the robot while the material is expanded in place to the outer wall. Most of the pipe is processed using tubular sections of a maximum allowable length that can traverse radius features while custom performs are delivered to areas with service and lateral tees and is processed separately. The following sections describe the robot design, material format, UV cure assessments, scarf joint design as well as all supporting mechanical and prototype experiments and testing in support of this effort.

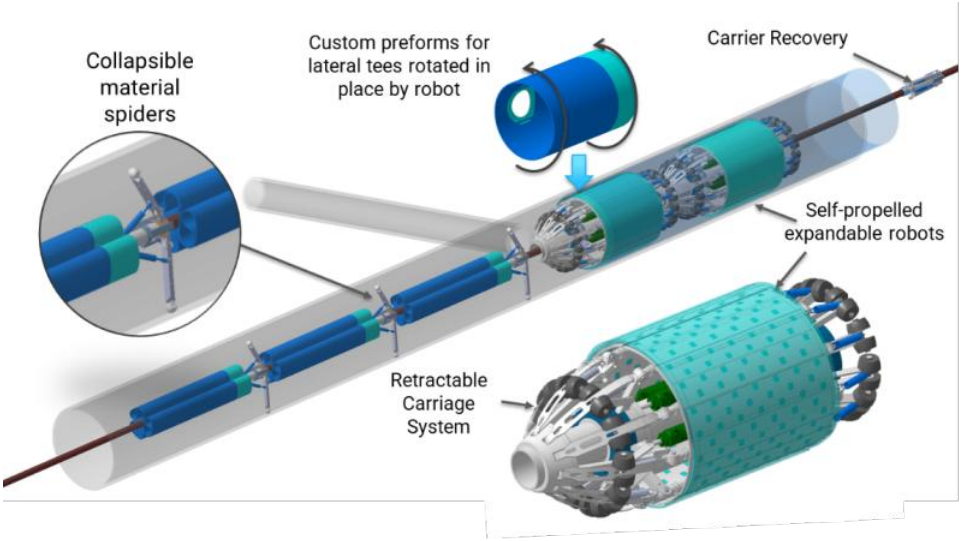

Figure 2 Self-Propelled Dual Robot iWrap System fed with discrete composite segments using a tethered feed supply and custom preform segments

1.1 Robot Design

The robotic system is a dual body self-propelled system using an inch-worm type motion where the rear robot when expanded and pushes the lead robot and vice-versa. The robot core body is collapsible for transport and to confirm to variation of pipe wall section with an open cross section to allow gas pass though. The conformable robot has an outer UV transparent bladder that inflates and cures the composite segments in place with an overlap between each composite segment. The rear robot hardware is nearly equivalent to the lead robot but can process custom preforms that have lateral openings. When collapsed, forward and aft rollers expand outwards thus suspending the bladder core for transport as shown in Figure 3(a) A connecting actuator then pushes the lead robot with the tail robot expanded and anchored to the already lined pipe wall.

This configuration is the most efficient propulsion method within corroded pipes with minimal risk of slip commonly observed for wheeled or track driven systems due to the large contact area and self-reaction condition. It also reduces the hardware and power requirements within the robot that only requires a local pneumatic source. Accurate registration of the robot for each material segment is achieved through independent motion of the robot driven and registered locally that captures the incoming segment pulled from the surface as it approaches the nose of the lead robot. As a result of this design, the overall power requirements for this system are low, as the robot only requires power to self-propel, expand and UV cure whereas the high energy requirements of material delivery is handled at the egress surface.

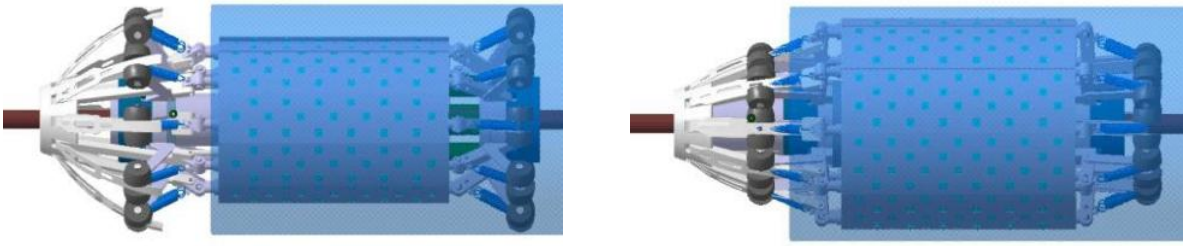

(a) (b)

Figure 3 (a) Robot in transport model (collapsed) and (b) expanded in place to consolidate and UV cure local pipe segment

A series of FE models were developed for the robotic system to determine the materials and dimensions of all internal support components to carry structural loading. These models optimized the supporting columns, bladder support structure as well as all linkage hardware as a function of bladder pressure. A buckling analysis was also conducted on all truss columns subjected to radial compression with the goal of minimizing robot mass. A minimal factor of safety of 1.5 was required and achieved for all internal elements up to an external bladder pressure of 200kPa (30psi). Critical buckling of the structure was not observed in the structure until pressures of 17MPa was applied (~2500psi).

1.2 Robotic Material Delivery

The core segments are delivered to the robot between two supporting truss segments, termed spiders, at each end of the collapsed form that prevent or minimize material contact to the pipe wall during transit as well as reduce tether friction forces. These spiders, shown in Figure 5, remain open during transport and can only be collapsed by the robot nose upon contact. They pass directly through the robot core while the material is expanded outward to the pipe wall. They comprise three articulating armatures that lock to an open state to support the material and tether. The armatures also include omnidirectional rollers that allow rotation of custom preforms by the robot for registration to lateral tees and service lines. The segment core acts a support structure for the material and both spiders and allows transmission of torque to the rear spider during rotation and registration. Several core architectures were evaluated for stiffness and torsional rigidity with a hollow wire braided tube with threaded end connections selected as the preferred configuration. The spider is also collapsed externally at the ingress and egress location to enable delivery of compact creel rolls of the preform material at the egress site. The process of material expansion by the robot causes a breakaway protective cover sheet to be removed at the head of the preform section exposing the uncured material to the already expanded pipe wall. This creates the joint

surface while also protecting the uncured material during delivery to the robot. A similar breakaway section is also present at the interior rear of each composite preform exposing that surface to the next material section. Static joint tension testing of those co-cured interfaces (flat panels of identical laminate thickness and scarf angles) was conducted to determine the optimal overlap and slope. The details are presented in a separate SAMPE paper [8]. Figure 4 also shows a tension test cell developed at CCM to test and evaluate spider and segment movement though straight and curved nominal 300mm diameter pipe sections (an omega geometry incorporating four 90º bends was also constructed with tests currently ongoing.)

Figure 4. Single Spider Segment with braided core that supports material while allowing rotation at the robot site

1.3 UV Array and Expandable Bladder Testing

The composite is UV cured using a network of 260 UV LEDs flush mounted on the robot in a series of overlapping sliding segments that allow collapse of the robot during transport while acting as the bladder reaction surface during expansion and pressurization. These support segments, shown in Figure 6, rotate about a pivot axis for expansion that can also pivot from front to rear of the robot on a network of ball joint attachments. This ensures that the robot substrate can support local section changes at pipe joints as well as at irregular cross sections. This self-reaction expansion design also ensures uniform application of pressure around the entire robot circumference while providing compliance that adapts to irregular cross sections. A variety of LED arrays arrangement configurations were tested to evaluate radiation uniformity at the 25mm standoff through the bladder to the composite surface. These arrays are also mounted on parallel heat sink substrates below the surface to dissipate heat at the diode to prevent burnout. A series of tests were done to ensure UV intensity uniformity over the surface of the bladder at the inflation standoff distance of approximately 25mm and a lateral spacing of approximately 20mm. This optimal spacing configuration was developed that provided between 150-200mW/cm^2 uniformly over the entire exposure area. The LED's have a max current rating of 1.4A per diode and 3.5VDC voltage drop resulting on 850W to drive each robot UV array. Infrared testing was also conducted for these arrays resulting in maximum steady state temperature of approximately 50°C at room temperature (Figure 6(b)).

The bladder material purchased from the DOW company is an optical grade and moldable silicone (SILATIC MS-1003). This material is non-linear elastic, has a strength of 5.5MPa, a high failure strain (325%) and an excellent level of UV transmittance. The bladder requires sustainable repeatable use in the repair process to allow expansion/cure of many sections prior to replacement.

In use, the silicone film of the bladder can experience a high level of strain during inflation and should survive cyclic loading/unloading conditions without any permanent deformation. To ensure this was a viable candidate for the iWrap process significant internal testing was conducted for strength and UV transparency under load.

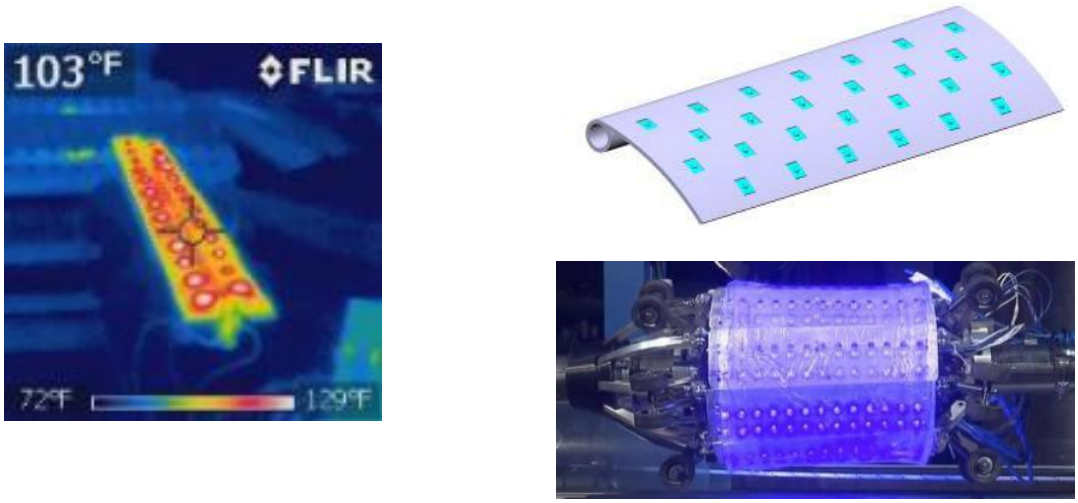

Figure 5 UV array panel IR testing of UV arrays iWrap robot with energized UV LED array

About 100g of two parts of silicon resin was mixed using a mix ratio of 1:1 by weight followed by degassing for ~15 minutes resin. The resin was then casted into a mold of 250mm by 250" with cavity height of 1mm. The resin was then cured at 150°C for 2 hours. Mechanical test samples were sliced from the cured film. The sample face was marked with black markers to capture the tensile strain of the sample during tensile loading using DIC. The sample was then mounted in the pneumatic grips of a mechanical test frame with 25mm gauge length. Tests were conducted at 50mm/min. Real time load was measured directly from the mechanical test frame and the average strain at the center was captured from the DIC system. For each sample, the dimensions (thickness and width) were measured prior to mechanical testing using a caliper. These dimensions were used to calculate the real time stress experienced by the sample. Stress-stain data was then generated for each sample and is shown in Figure 7. Stress-strain results were obtained from tensile testing on 5 silicone film samples. The UV transparent silicon film samples exhibited on average of 314% and 4.5MPa for failure strain and strength, respectively.

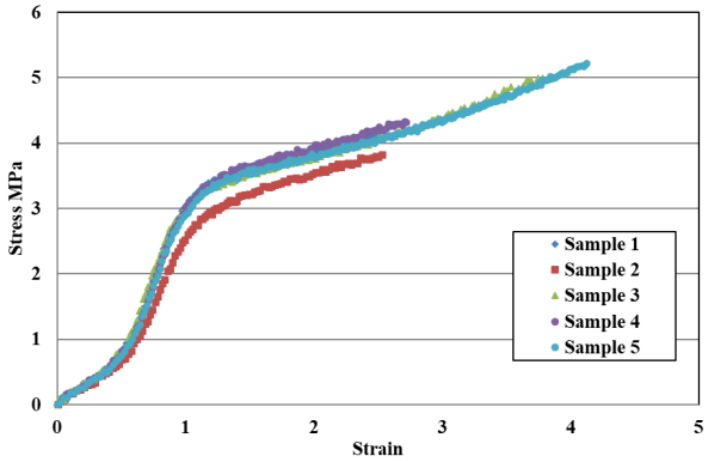

Figure 6. Stress-strain results obtained from tensile testing on 5 silicone bladder film samples.

Cyclic loading/unloading tests were also conducted to access the durability of the bladder with increasing strain application (Figure 8). This sequence of testing was also intended to measure the limit in tensile strain that would not exhibit any permanent deformation. Samples were mounted and exposed to number of load/unload cycles with 25% strain increase interval until failure. Tests were conducted at crosshead speed of 50 mm/min and a gauge length of 25mm. For each sample, the real time load-strain data was collected. From this data the failure strain, strength, residual strain, and number of cycles until failure were quantified and listed in Table 1. It is noteworthy that the residual strain was captured from the last complete load/unload cycle. These results reveal the following observations: On average the samples exhibit a strength of ~3.7GPa, a failure strain 353% and negligible residual strain (~2.3%). Overall, the cyclic loading/unloading test results indicates that the silicone film can maintain its elasticity during cyclic loading until failure. To confirm this, the dimensions of the sample were compared before after tensile loading up to the highest strain level with no measurable change in sample dimensions.

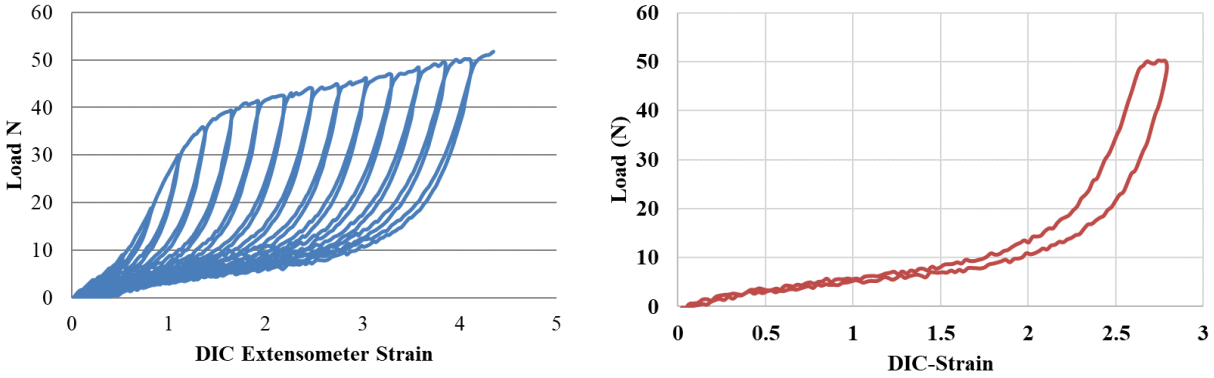

Figure 7 Typical Load/unload cycles till failure (left) and last complete cycle before failure. Last cycle shows negligible residual strain (0.026).

Table 1. Failure strain, strength and residual strain and number of cycles till failure obtained from cyclic loading/unloading tests. The width of each sample was 12.5mm.

	Thickness (mm)	Strain at failure	Strength (MPa)	Residual strain	No. of Cycles
Sample#1	0.932±0.038	372%	3.18	0%	15
Sample#2	1.00±0.008	434%	4.13	2.6%	17
Sample#3	0.978±0.008	267%	4.10	0.2%	11
Sample#4	0.854±0.029	339%	3.53	5%	14

Transmitted intensity through the silicone film (~1 mm thickness) was measured and normalized by the intensity without sample. The thickness across 3 samples was measured at 3 different locations and the normalized intensity was calculated. Across all samples the thickness average is 1.17 mm with a standard deviation of 0.054 mm. The normalized transmitted intensity 96.8% with a standard deviation of 0.4%.

To assess the optical performance of the bladder during stretching the transparency of a strained silicon film was investigated. A silicon film with a thickness of 1mm and a width of 25.4 mm, was mounted in the Instron and loaded in tension at 50mm gauge length and 50mm/min crosshead speed. A UV light meter was fixed behind the sample and a 400nm UV light source was placed in front. The real time transmitted intensity was measured during the tensile loading and

then, the data was normalized by the intensity without sample. It was observed that the average normalized transmitted UV light is at 92.8 %, while the intensity never dropped below 91% This shows that even under large strains the transmittance can be maintained so this grade of silicone was deemed suitable for the repair process. A process to fabricate a UV transparent bladder annulus was developed internally that integrated an internal valve connector for pressurization. Three bladder prototypes were fabricated and tested with the final design incorporated into the final robot prototype.

2. UV MATERIALS AND TESTING

2.1 Material Format

E-glass fiber 7781-style fabric was selected and supplied by supplied by Fibre Glast Developments Corporation. The weight of the fabric is 305-345.8g/m^2 and thickness ranges from 0.2032mm to 0.2048mm. The 7781 style E-glass is an 8-harness satin weave fabric; the fiber tow in the warp or longitudinal direction (0 degree) travels over 7 fiber tows and under 1 tow in the weft or fill direction (90 degree). The polymer resin (Sunrez 7310) was supplied by Sunrez Corporation. The composite preforms are manufactured by wet winding 610mm wide fabrics on a filament winder over a multi segment removable mandrel that collapses allowing for retrieval of the uncured laminate (Figure 9). A UV transparent film is used as the core substrate with an outer bag wrapped post process (the outer diameter film is intended to provide UV protection during storage while both films protect the preforms from contamination during transport within the pipe). The preform is then placed in a stage that collapses the preform to a compact section as shown below. This reduces the 305mm diameter section down to 130mm outer diameter allowing for insertion and transport to the robot. A variety of forms were evaluated with the clover shape being selected as a suitable shape as a collapsed preform. The collapsed preform is then placed on a flexible traveler core with a final wrap tape added to confine the collapsed shape. The pipe design uses 18 layers of the 7781 E-glass fabric (50% FVF) with a consolidated wall thickness of 4.4mm (0.175in).

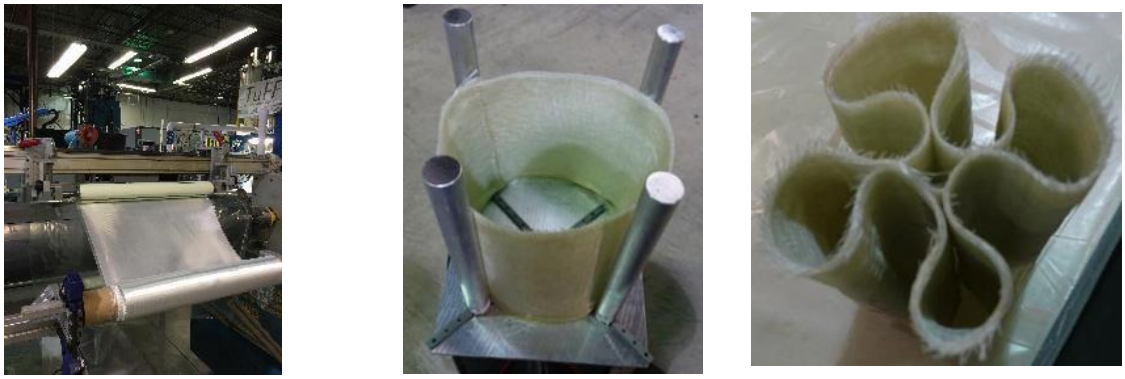

Figure 8. Wet winding of 8-harness fabric followed by extraction and collapse into compact preform.

2.2 Material Testing

The mechanical and thermal properties of VARTM infused 7781 E-Glass fabric with Sunrez 7310 was evaluated as part of this effort (in production a prepreg process would be used to impregnate the fabric).The 2.25mm panels were UV-cured for 2.5 minutes to ensure full cure

through the thickness with typical composite panels and C-scans shown in Figure 10. The UV curing assessment of this resin was evaluated and is discussed in a later section. Tensile and compression testing in warp and weft direction was performed in an Instron 5985 at the constant displacement rate of 1.27mm/min. V-notch samples for in-plane shear properties were tested in one direction. The density (1.9 g/cm^3), void content (0.6%), and fiber volume fraction (49.25%) of the composite panel were measured according to ASTM D2734-16 [9].

The longitudinal tensile stress-strain curves exhibited linear elastic behavior up to failure. The failure modes of the broken samples were classified based on the ASTM D3039-17 [10]. The failure area of all the samples was near the grip. Additional testing is planned to assess microcracking onset strains, resin properties and fiber-resin adhesion. Alternate sizings applied to the fibers are offered by Hexcel (supplier of the fabric) and are currently being accessed through fiber-matrix interface testing at UD-CCM.

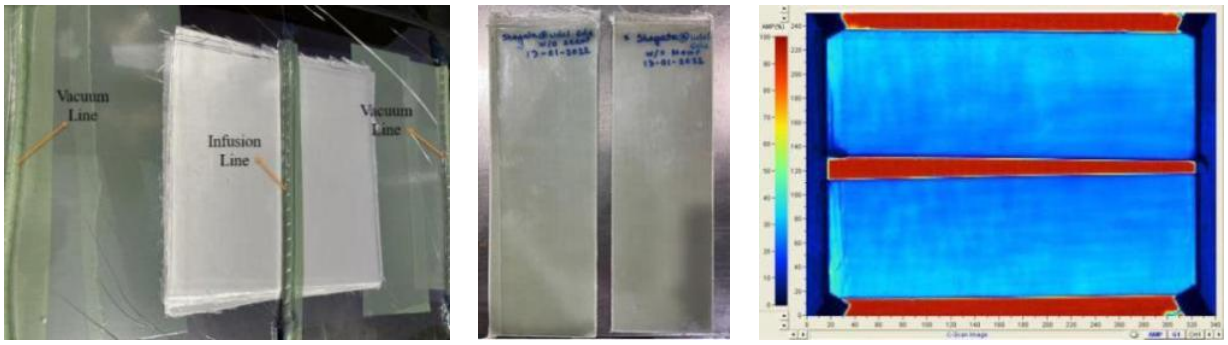

(a) (b) (c)

Figure 9. (a) Resin Infusion, (b) fabricated panels and (c) c-scans of 7781 E-Glass/Sunrez 7310

Table 2. Properties of Sunrez 7310 & E-glass 7781 Composite

Loading	Direction	Property	Average	SD	CV
Tension D3039	Warp 5 Samples	Modulus (Msi)	3.37	0.233	6.92%
		Strength (Ksi)	50.19	3.68	7.33%
		Strain	1.60%	0.08%	5.00%
		Poisson ratio	0.1	0.009	9.07%
	Weft 6 Samples	Modulus (Msi)	3.35	0.063	1.87%
		Strength (Ksi)	43.02	2.78	6.47%
		Strain	1.51%	0.10%	6.46%
Compression D3410	Warp 5 Samples	Modulus (Msi)	4.27	0.07	1.56%
		Strength (Ksi)	54.87	1.41	2.58%
		Strain	1.28%	0.11%	8.88%
	Weft 5 Samples	Modulus (Msi)	4.18	0.04	1.05%
		Strength (Ksi)	43.38	1.98	4.55%
		Strain	1.07%	0.02%	2.01%
V Notch Shear D5379	Warp 5 Samples	Modulus (Msi)	0.54	0.036	6.80%
		Strength (Ksi)	8.74	0.4	4.61%
		Strain	8.49%	1.69%	19.85%
	Weft 5 Samples	Modulus (Msi)	0.76	0.14	18.7%
		Strength (Ksi)	8.92	0.16	1.82%
		Strain	8.65%	1.62%	18.75%

Average, standard deviation and coefficient of variation of the mechanical properties are tabulated in Table 2. An almost 20% reduction in average strength numbers is seen in the weft samples which is comparable to strength reductions observed in the literature [11]. The higher

strength direction is used in the axial direction of the pipe that is more highly loaded (due to pipe bending spanning scoured soil while being subjected to dead and live loads). Tensile strains to failure are around 1.5%-1.6% (an order of magnitude higher than steel) but further improvements are expected, with appropriate selection of sizing compatible with the UV resin, to improve fiber-resin adhesion. Fatigue testing is planned in the future.

2.3 Thermal Characterization

Cured Sunrez 7310/E-glass 7781 panels were conditioned to evaluate the Tg of the resin in a typical pipe environment to ensure that the resin meets service temperature requirements. The composite was immersed in water at 30°C for 2 weeks to produce "wet" samples. Additional samples were kept in a desiccator for two weeks at ambient temperature to produce the "dry" sample. Dynamic Mechanical Analysis (DMA) tests that were conducted to evaluate the Tg: "Dry Test", "Wet/Dry Test" and "Wet/Immersed Test". The "Dry Test" used the "dry" sample run in the DMA using dry purged gas. The "Wet/Dry Test" used the "Wet" sample run in the DMA using dry purge gas. The "Wet/Immersed Test" used the "wet" sample run in the DMA while immersed in water.

DMA tests were run using three point bending with a 40mm length between fixed support points using a 1% strain amplitude based on the thickness of the sample. The samples were nominally 2.2 mm thick and 12.6 mm wide. All tests were run at 10 Hz, which is the Netzsch DMA default setting. The immersion tests were run at 0.1 °C/min, due to the high thermal mass of the water tank. All other tests were run at 2 °C/min in the Netzsch DMA convection furnace.

ASTM D7028 section 12.1 was used to measure the "Tg-onset" of the drop in the storage modulus [12]. The dry-dry, wet/dry, and wet/immersed test Tg onset were measured at 108°C, 57°C and 52°C respectively which is nearly double the temperature needed for the expected service temperature range for this application. In summary, the Sunrez 7310 resin was deemed suitable for use as the UV curable pipe polymer in the repair process.

2.4 Light Attenuation and Cure Characterization

A UV-DSC analysis of a Sunrez 7310 sample showed that the surface of the neat resin was cured within 5 sec using an exposure intensity of 36 mW/cm^2 for a total UV energy ($E_{UV\text{-}cure}$) of 180mWs/cm^2. Assuming equivalent exposure on the back side of the composite, the cure time was estimated based on dosage and attenuation through the material. The intensity as a function of thickness can be expressed with Beer-Lambert law (Eqn. 1) where I_0 is the initial intensity, α is the coefficient of attenuation and z is the thickness of the material [13].

$$I(z) = I_0 \cdot e^{-\alpha \cdot z} \quad [1]$$

The coefficient of attenuation was measured for panels with different fiber volume fraction (neat resin, 34% FVF, 53% FVF). Thicknesses were varied and the light intensity measured after cure as shown in Figure 11. The intensity of the 400nm high power LED was adjusted for each material to stay within the sensor range. A linear curve fit with the intensity plotted in the logarithmic scale provides us the best fit parameter of the coefficient of attenuation of the materials and is shown in Table 3.

A linear intensity plot (Figure 11(a)) illustrates the rapid reduction in intensity as a function of thickness over a typical range of panel thicknesses. The thickness is designed to meet all load requirements established the design studies but has a direct impact on the time needed to fully cure

the part. Minimum gauge thickness designs allow lower preform mass to be transported to the PIP repair area and reduce indexing time to fee and cure composite preforms.

Table 3. Coefficient of attenuation for different fiber volume fractions.

Material	Fiber volume fraction	Coefficient of attenuation [1/mm]
Sunrez 7310 (resin)	0%	0.40
E-glass 7781 / Sunrez 7310	34%	0.72
E-glass 7781 / Sunrez 7310	52%	0.95

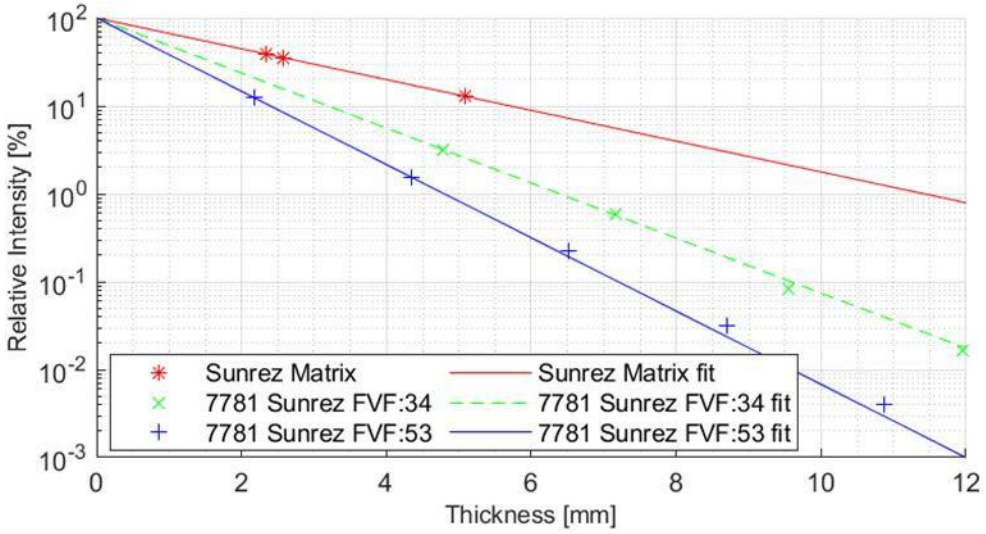

Figure 10. Linear best fit of experimental obtained light intensity obtains the UV-light attenuation in our proposed composite solution

The cure time will exponentially increase with thickness and must be taken into consideration for total repair time as design thickness increases. To evaluate this , an 18-layer laminate was vacuum infused with a total thickness of 4.4 mm. Prior to UV exposure the panel was covered with a UV blocking sheet. This sheet was moved in controlled time intervals and the hardness of the top and bottom side was measured and is plotted in Figure 11(b). The predicted cure time based on the required UV-light energy of 180mWs/ cm^2 is around 77 sec. Top and bottom hardness are starting to converge at approximately 80 seconds indicating similar uniform cure of both surfaces. Additional experiments for thicker laminates and layups including the final design are planned to establish standard operating procedures for UV cure for performs of various thickness.

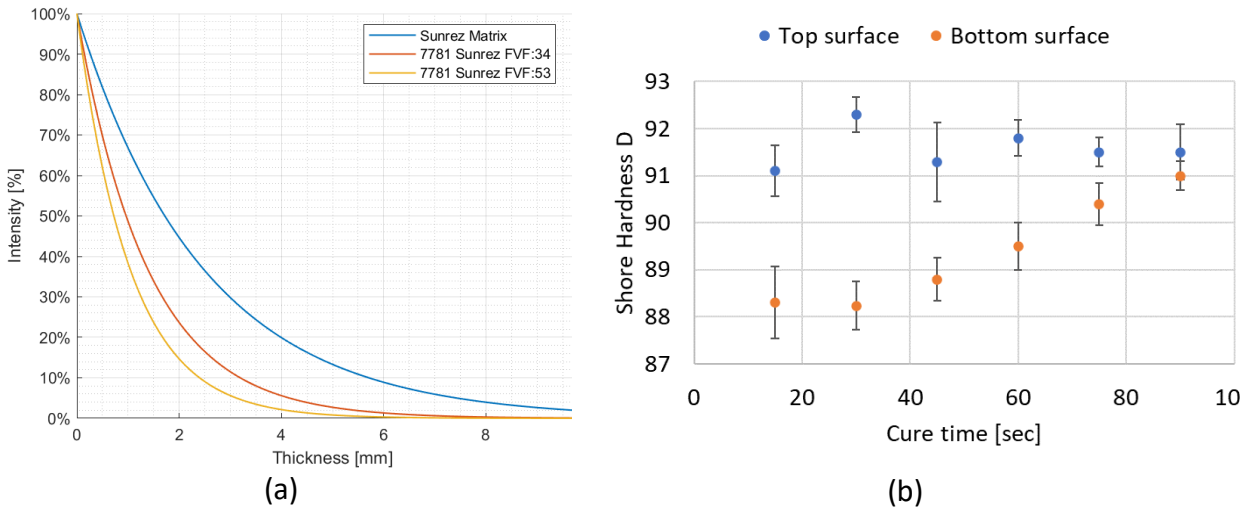

Figure 11. (a) UV- light Intensity as a function of thickness (b) hardness test for a 4.4 mm laminate showing a cure time of approximately 80-90s comparing well with light intensity approach.

2.5 Scarf Joint Testing

The scarf joint between discrete sections bonded within the pipe requires significant testing to determine the optimal design configuration. Very little data is available for scarf joints using UV cure resins. Several different joint configurations were tested with results of that study presented here [8]. The average tensile strength vs scarf angle showed that that the tensile strength of the scarf joint approached that of the baseline material at low angle as expected (100% translation of laminate tensile strength). All scarf angles studied exceeded the expected pipe design stress level of 48.2Mpa (7 ksi) providing safety factors ranging from 4-7 [8].

2.6 Structural Monitoring and Damage Detection for Gas Leakage

Long-term gas service can lead to the transverse microcracking and delamination of the laminates due to quasi-static or fatigue damage. Since it is well known that connected crack path can make acute gas leakage [14], predicting the point when an initial microcrack will be created is required through the evaluation of the strain amplitude or fatigue cycle. Adsorption of natural gas molecules saturated into the composite pipelines changes the baseline resistance of the sensing layers along with the influence of the temperature fluctuation and moisture content. Prior work at UD-CCM established distributed carbon nanotube (CNT) networks for detecting the onset and accumulation of damage in composites [15] [16]. This work has been extended here to using this technology to detect methane gas in the air atmosphere. Glass fiber random veils with an areal density of 10 g/m^2 was used as the substrate for functionalized carbon nanotube (CNT) coatings to fabricate sensing composites, considering the ultra-violet (UV) transmittance. A manufacturing process was developed at UD-CCM, and the CNT coated sensing fabric exhibited the baseline electrical resistance ranging from 100 to 300 kΩ. Figure 13(a) shows the schematics of setup to test the sensing fabrics for gas sensing applications. Methane and air tanks were connected to a tube furnace equipped with gas flow controllers, and the sensing fabric was hermetically wired with resistance monitoring system. The electrical response was recorded while the air and methane gas were cycled within the tube furnace.

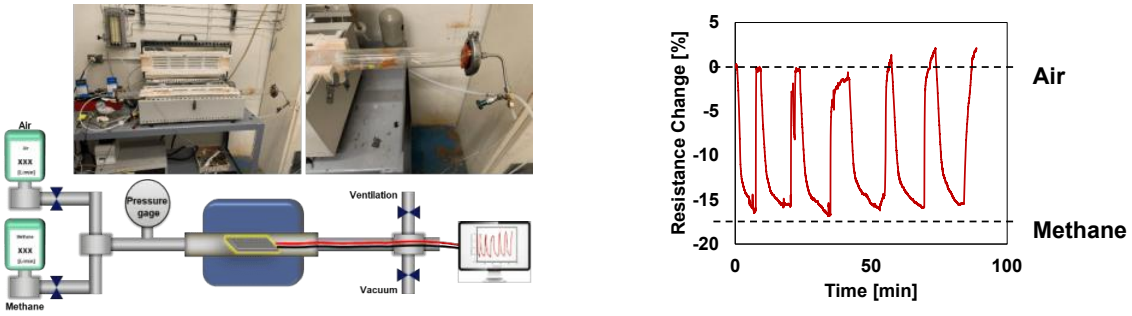

Figure 12 (a) Set-up to test CNT coated textiles for gas sensing applications and (b) resistance change of carbon nanotube nanocomposite sensors while cycling between air and methane gas.

Figure 13(b) shows the electrical response of CNT coated sensing fabric with respect to the change of gas species between air and methane. The resistance measured in the air atmosphere was used as the baseline. As the methane gas was periodically on and off, 17% decrease in resistance was observed. The depleted electrons by the oxygen species are released as the nanotube surfaces are exposed to reducing gases like methane, which lead to an increase in the conductance [17]. It was shown that the sensing fabric has a potential to be utilized as methane detectors embedded in the gas pipelines along with their structural health monitoring capabilities reported in the literature. [15] [16].

3. TUBE MANUFACTURING

Several 305mm composite preforms were expanded, consolidated and UV cured both freestanding and inside transparent 305mm diameter plastic pipe section to observe the evolution of contact between the composite and the pipe wall and prove-out feasibility of the iWrap process (Figure 14(a)). With full power, a cure time of less than 5 minutes was observed on the outer wall indicating full cure within the tube the structure. Some wrinkling was observed on the outer plies of the confined tube as the circumferential length of outer layers of the preform were slightly longer than the pipe ID in our first prototypes. This can be resolved using the measured cure ply thickness from the pipe wall and modifying the mandrel dimensions. Free standing pipe sections (i.e. self-reacts the bladder pressure without contact with the steel pipe wall) were also manufactured with success showing that this process is viable for pipe repair within damaged pipe sections or across open gaps such as condensate pots. This approach eliminates wrinkling issues. Free standing trials demonstrated the feature of our repair system to bridge gaps that exist in cast iron pipe joints using self-reacting preforms that do not require contact with the pipe wall for consolidation. Further trials are ongoing that look at how the system can traverse and line complex pipe sections such as and expansion joint recently fabricated at UD-CCM (Figure 15) This hardware is used to understand how the spiders with preforms navigate the pipe under tether tension while also evaluating robot hardware navigation.

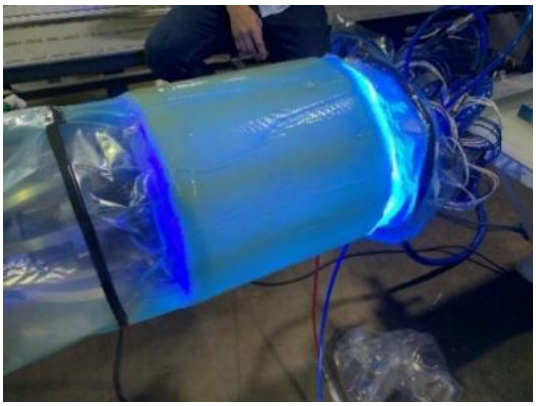

(a)

(b)

Figure 13 (a) UV Cure of 305mm Pipe Sections with the iWrap robot (b) first cured composite section removed from pipe for inspection

(a)

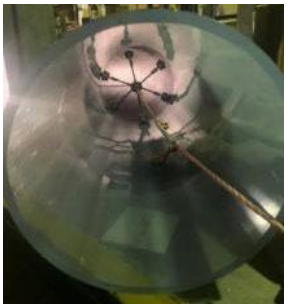

(b)

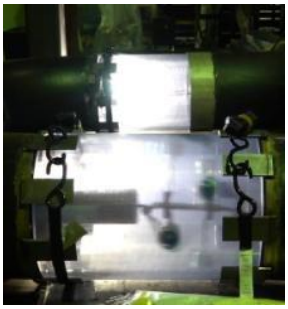

(b)

Figure 14 (a) Expansion Joint section to test tether, (b) spiders, and (c) material transport.

4. CONCLUSIONS

The UD-CCM process is a novel repair process for pipeline repair that offers rapid rehabilitation of degraded gas pipeline infrastructure without shutoff of service. This paper demonstrates that composite preforms can be manufactured on the surface, transported to an underground robot, expanded, and cured in place. A suitable UV transparent bladder was developed and demonstrated on the robot and a viable UV polymer and glass fabric system was tested and proven as a suitable candidate material for structural pipeline repair. Key results show joint strength with over 80% joint efficiency (compared to axial tensile strength) that exceed design stress levels by 7-fold, retention of joint strength is achieved with UV cure to a cured substrate and that the joint lengths can be dramatically reduced while providing greater tolerance for assembly during repair. We have also demonstrated a CNT distributed sensor for gas leak detection that can be integrated into future composite pipe structures for lifecycle monitoring.

5. ACKNOWLEDGEMENTS

The authors wish to acknowledge the funding and support from the Dept. of Energy ARPA-A DE-FOA-0002289, Rapid Encapsulation of Pipelines Avoiding Intensive Replacement (REPAIR) program.

6. REFERENCES

[1] Chapetti et.al., "Full scale experimental analysis of stress states in sleeve repairs of gas pipelines," *International Journal of Pressure Vessels and Piping,* p. 78–87, 2001.

[2] P. G. Dixon, T. Tafsirojjaman, J. Klingaman, M. H. Hubler, S. Dashti, T. D. O'Rourke, K. Farrag, A. Manalo and B. P. Wham, "State-of-the-Art Review of Performance Objectives for Legacy Gas Pipelines with Pipe-in-Pipe Rehabilitation Technologies," *Journal of Pipeline Systems Engineering and Practice,* vol. 14, May 2023.

[3] Office of Energy Policy and Systems, "Natural Gas Infrastructure Modernization Programs at Local Distribution Companies: Key Issues and Considerations," US DOE, 2017.

[4] Y. J. Jung and S. K. Sinha, "Evaluation of Trenchless Technology Methods for Municipal Infrastructure System," *Journal of Infrastructure Systems,* vol. 13, p. 144–156, June 2007.

[5] S. T. Ariaratnam, J. S. Lueke and E. N. Allouche, "Utilization of Trenchless Construction Methods by Canadian Municipalities," *Journal of Construction Engineering and Management,* vol. 125, p. 76–86, 1999.

[6] Koch et.al., "Corrosion cost and preventative strategies in the United States," Federal Highway Administration, Office of Infrastructure Research and Development, 260–311, 2001.

[7] J. A. McElligott, J. Delanty and B. Delanty, "Use of hot taps for gas pipelines can be expanded," *Oil and Gas Journal,* vol. 96, 1998.

[8] S. Das, J. W. Gillespie Jr, H. Shenton III and J. Tatar, "Mechanical Behavior of UV-Cured Composite Stepped Lap Adhesive Joints," *SAMPE Conf.,* 2023.

[9] D2734-16, *Test Methods for Void Content of Reinforced Plastics,* ASTM International.

[10] D3039, *Test Method for Tensile Properties of Polymer Matrix Composite Materials,* ASTM International.

[11] Composite Materials Handbook, Mil-hbk 17, Dept. of Defence Handbook.

[12] D7028, *Test Method for Glass Transition Temperature (DMA Tg) of Polymer Matrix Composites by Dynamic Mechanical Analysis (DMA),* ASTM International.

[13] I. Saenz-Dominguez, I. Tena, M. Sarrionandia, J. Torre and J. Aurrekoetxea, "An analytical model of through-thickness photopolymerisation of composites: Ultraviolet light transmission and curing kinetics," *Composites Part B: Engineering,* vol. 191, p. 107963, June 2020.

[14] H. Kumazawa and J. Whitcomb, "Numerical Modeling of Gas Leakage Through Damaged Composite Laminates," *Journal of Composite Materials,* vol. 42, p. 1619–1638, August 2008.

[15] E. T. Thostenson and T.-W. Chou, "Carbon Nanotube Networks: Sensing of Distributed Strain and Damage for Life Prediction and Self Healing," *Advanced Materials,* vol. 18, p. 2837–2841, November 2006.

[16] E. T. Thostenson and T.-W. Chou, "Real-time in situ sensing of damage evolution in advanced fiber composites using carbon nanotube networks," *Nanotechnology,* vol. 19, p. 215713, April 2008.

[17] A. Amutha, S. Amirthapandian, A. K. Prasad, B. K. Panigrahi and P. Thangadurai, "Methane gas sensing at relatively low operating temperature by hydrothermally prepared SnO2 nanorods," vol. 17, 2015.